Nonlinear elastic analysis of laterally loaded piles

Bipin Kumar Gupta & Dipanjan Basu
Department of Civil & Environmental Engineering,
University of Waterloo, Waterloo, Ontario, Canada

ABSTRACT
The objective of this paper is to describe a new continuum-based analysis for predicting the nonlinear response of pile foundations, subjected to static lateral loads. In the analysis, the pile is modeled as an elastic Euler-Bernoulli beam and the soil as a continuum with nonlinear elastic properties that is described by a modulus degradation relationship. The soil displacements are assumed to be a product of separable functions and the principle of virtual work is applied to obtain the governing differential equations describing the pile and soil displacements, which are solved numerically using the one-dimensional finite difference method, in an iterative scheme. The reliability of the results obtained from the present analysis is verified with the results equivalent 3-D finite element analysis.

RÉSUMÉ
L'objectif de cet article est de décrire un nouveau continuum basé analyser pour prédire la réponse non linéaire des fondations de pieu, soumis à des charges statiques de difuso. Dans l'analyse, la pile est modélisée comme un faisceau Euler-Bernoulli élastique et le sol comme un continuum avec propriétés d'élasticité non linéaires qui est décrite par une relation de dégradation du module. Les déplacements du sol sont considérées comme un produit de fonctions séparables et le principe des travaux virtuel est appliqué pour obtenir les équations différentielles décrivant les déplacements de pile et le sol, qui sont numériquement de riposter en utilisant la méthode des différences épicycloïdes unidimensionnel, dans un schéma itératif. La fiabilité des résultats obtenus de la présente analyse est vérifiée avec l'analyse par éléments finis 3D équivalent de résultats.

1 INTRODUCTION

Structures like tall buildings, transmission towers, oil and gas platforms, and wind turbines have piles as their foundation elements that are subjected to large lateral loads from wind, waves, water currents, and traffic. An interest in the analysis of such pile foundations lies in the prediction of nonlinear pile response subjected to the aforementioned lateral loads.

In the geotechnical foundation engineering practice, the *p-y* method (Reese et al. 1975, O'Neill et al. 1990, Zhang and Ahmari 2013) is widely used by engineers to predict the nonlinear response of these laterally loaded piles. The *p-y* method for the analysis and design of laterally loaded piles is also included in the API (2011) design code of practice. However, there are a few limitations to the *p-y* method (i) the *p-y* curves are modeled as uncoupled springs and are characterized by the spring constant *k* (compressive resistance of the soil) along the pile-shaft, they do not account for the shear transfer (characterized by *t*) between adjacent soil layers; thus, neglecting the continuum nature of the pile-soil interaction problem, (ii) the *p-y* curves reported in the aforementioned design code were developed from a few full-scale field pile-load tests and they are site-specific, and (iii) parameters such as the ε_{50} used for stiff clay (Reese et al. 1975) criterion for the development of *p-y* curves is empirical and arbitrarily determined by users based on experience. The continuum-based methods with FE or FD solution techniques (Baguelin et al. 1977, Kooijman 1989, Trochanis et al. 1991, Achmus et al. 2009) using commercially available software's or self-developed codes used by several researchers can handle various geometry, boundary conditions, and elastic-plastic constitutive models and can be used to predict the nonlinear response of piles accurately and realistically. However, their use in the design is limited because of (i) the modelling knowledge required to develop such solution techniques or the expertise to use a particular software and (ii) such techniques require considerably large computational effort. The FE software's (e.g., ABAQUS) facilitate the use of sophisticated constitutive models based on elasticity and plasticity theory to model the nonlinear soil behaviour; however, such models based on plasticity theory are only useful when the design interest is the estimation ultimate load capacity. For laterally loaded pile problems the primary interest in design is the estimation of head response under working load conditions (e.g., head displacement and rotation is often the design criterion); thus, the use of such sophisticated constitutive models based on plasticity theory might not be necessary.

In this paper, a new method is developed for the analysis of laterally loaded pile foundations subjected to a static force and/or moment at the pile-head. In the analysis, the pile is assumed to be an elastic Euler-Bernoulli beam and the soil is characterized by a nonlinear elastic relationship, available in the literature. The displacement within the soil mass is considered to be a product of separable functions and the principle of virtual work is applied to obtain the governing differential equations describing the pile and soil displacements which are solved using a 1-D FD scheme. The results obtained from the analysis are verified with the results of equivalent 3-D FE.

2 NONLINEAR ELASTIC SOIL MODEL

The degradation of soil modulus with strain (nonlinear soil behaviour) can be expressed as a ratio of G_s/G_{s0} where G_s is the secant shear modulus at any strain and G_{s0} is

the initial (linear elastic or small-strain) shear modulus. In this paper, the nonlinear elastic soil model developed by Osman et al. (2007) expressed in the form of a power-law (Eq. [1]) is used, which is given by

$$G_s = G_{s0}\left(\frac{\varepsilon_q}{\varepsilon_{q0}}\right)^b \quad [1]$$

where

$$\varepsilon_q = \sqrt{\frac{2}{9}\left[\left(\varepsilon_{rr}-\varepsilon_{\theta\theta}\right)^2+\left(\varepsilon_{\theta\theta}-\varepsilon_{zz}\right)^2+\left(\varepsilon_{zz}-\varepsilon_{rr}\right)^2\right]+\frac{4}{3}\left(\varepsilon_{r\theta}^2+\varepsilon_{\theta z}^2+\varepsilon_{zr}^2\right)} \quad [2]$$

ε_q is the deviatoric strain, ε_{rr}, $\varepsilon_{\theta\theta}$, ε_{zz}, $\varepsilon_{r\theta}$, $\varepsilon_{\theta z}$, and ε_{zr} are the strain components for a 3-D strain state in soil for a r-θ-z coordinate system, ε_{q0} is the maximum deviatoric strain of linear elastic behavior at ~ 10^{-5}, and b (= – 0.5) is a curve fitted parameter describing the nonlinear variation of soil with deviatoric strain.

3 FORMULATION

3.1 Problem definition

Figure 3 shows a circular pile embedded in a multi-layered nonlinear elastic soil deposit where the pile is assumed to be an elastic Euler-Bernoulli beam of length L_p, radius r_p, area of cross-section A_p, second moment of inertia I_p, and characterized by Young's modulus E_p. The soil layers are characterized by the modulus degradation relationship given by Eq. [1]. Each soil layer extends to an infinite distance along the radial and the n^{th} soil layer extends to an infinite distance in the vertical direction. A cylindrical r-θ-z coordinate system is chosen for the purpose of analysis where the origin of the coordinate system lies at the centre of the pile-head. Further, in the analysis, no slippage or separation between the pile and the surrounding soil is assumed. The objective of the analysis is to predict the nonlinear pile response–displacement (w) and rotation (dw/dz) under the application of the static horizontal force F_a and/or moment M_a at the pile-head.

3.2 Soil displacement, strain, stress-strain functions

The horizontal soil displacement generated by the pile displacement $w(z)$, is described as a product of separable functions. The effect of vertical soil displacement u_z for laterally loaded pile analysis is assumed negligible (Nogami and Novak 1977). Thus, the radial u_r and tangential u_θ displacements are mathematically expressed as (Basu et al. 2009, Gupta and Basu 2017)

$$u_r(r,\theta,z) = w(z)\,\phi_r(r)\cos\theta \quad [3]$$

$$u_\theta(r,\theta,z) = -w(z)\,\phi_\theta(r)\sin\theta \quad [4]$$

where ϕ_r and ϕ_θ are dimensionless functions of the radial coordinate that are both assumed to be equal to 1.0 at $r = r_p$ and are both assumed to be equal to zero at $r = \infty$. The sine and cosine functions ensure that the variation of the soil displacements in the tangential direction is compatible with the horizontal pile displacement.

Using the soil displacement field, the infinitesimal soil strains (with contractive strains assumed positive) is expressed as

$$\begin{bmatrix}\varepsilon_{rr}\\ \varepsilon_{\theta\theta}\\ \varepsilon_{zz}\\ \varepsilon_{r\theta}\\ \varepsilon_{rz}\\ \varepsilon_{\theta z}\end{bmatrix} = \begin{bmatrix} -w(z)\dfrac{d\phi_r(r)}{dr}\cos\theta \\ -w(z)\dfrac{\phi_r(r)-\phi_\theta(r)}{r}\cos\theta \\ 0 \\ \dfrac{1}{2}w(z)\left\{\dfrac{\phi_r(r)-\phi_\theta(r)}{r}+\dfrac{d\phi_\theta(r)}{dr}\right\}\sin\theta \\ -\dfrac{1}{2}\dfrac{dw(z)}{dz}\phi_r(r)\cos\theta \\ \dfrac{1}{2}\dfrac{dw(z)}{dz}\phi_\theta(r)\sin\theta \end{bmatrix} \quad [5]$$

Further, using the stress-strain relationship, the stress state at any point within the soil mass is given by

$$\sigma_{pq} = \lambda_s \delta_{pq}\varepsilon_{ll} + 2G_s\varepsilon_{pq} \quad [6]$$

where σ_{pq} and ε_{pq} are soil stress and strain tensors and the summation is implied by the repetition of the indices p and q, ε_{ll} is the volumetric strain, and δ_{pq} is the Kronecker's delta.

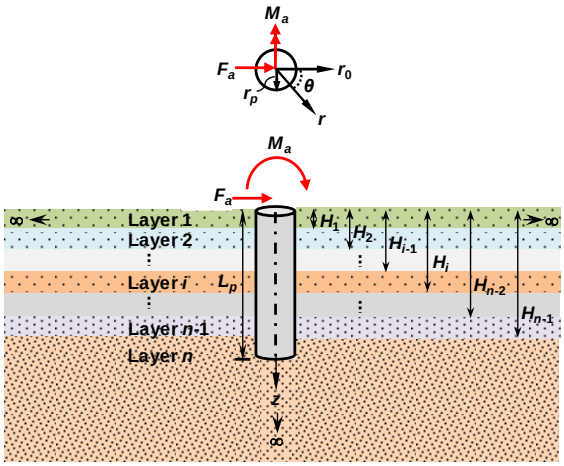

Figure 1. Laterally loaded pile in a multilayered nonlinear elastic soil deposit

3.3 Application of principle of virtual work

Applying the principle of virtual work to the pile-soil system (Figure 1) the following equation is obtained

$$E_p I_p \int_0^{L_p} \left(\frac{d^2w}{dz^2}\right)\delta\left(\frac{d^2w}{dz^2}\right)dz + \int_0^{\infty}\int_0^{2\pi}\int_{r_p}^{\infty} \sigma_{pq}\delta\varepsilon_{pq} r dr d\theta + \int_{L_p}^{\infty}\int_0^{2\pi}\int_0^{r_p} \sigma_{pq}\delta\varepsilon_{pq} r dr d\theta$$
$$-F_a\,\delta w\big|_{z=0} + M_a\delta\left(\frac{dw}{dz}\right)\Big|_{z=0} = 0 \qquad [7]$$

where the first, second, and third integral on the left-hand side of Eq. [7] denotes the internal virtual work done by the pile, the soil except the cylindrical soil domain below the pile base, and the cylindrical soil domain of radius r_p below the pile base, respectively. The fourth and the fifth term on the left-hand side of Eq. [7] denotes the external virtual work done by the applied force and moment, respectively.

Substituting Eqs. [5] and [6] in Eq. [7] and introducing layering, the following equation is obtained

$$\sum_{i=1}^{n}\int_{H_{i-1}}^{H_i} E_p I_p \left(\frac{d^2w_i}{dz^2}\right)\delta\left(\frac{d^2w_i}{dz^2}\right)dz + \int_{L_p}^{\infty}\pi r_p^2 G_{sn0}\left(\frac{dw_{n+1}}{dz}\right)\delta\left(\frac{dw_{n+1}}{dz}\right)dz$$
$$+\sum_{i=1}^{n}\int_{H_{i-1}}^{H_i}\int_0^{2\pi}\int_{r_p}^{\infty}\Bigg\{\left(\lambda_{si}+2G_{si}\right)\left(\frac{d\phi_r}{dr}\right)^2\cos^2\theta + 2\lambda_{si}\frac{d\phi_r}{dr}\left(\frac{\phi_r-\phi_\theta}{r}\right)\cos^2\theta$$
$$+\left(\lambda_{si}+2G_{si}\right)\left(\frac{\phi_r-\phi_\theta}{r}\right)^2\cos^2\theta + G_{si}\left(\frac{\phi_r-\phi_\theta}{r}\right)^2\sin^2\theta$$
$$+2G_{si}\frac{d\phi_\theta}{dr}\left(\frac{\phi_r-\phi_\theta}{r}\right)\sin^2\theta + G_{si}\left(\frac{d\phi_r}{dr}\right)^2\sin^2\theta\Bigg\} w_i\delta w_i\, r dr d\theta dz$$
$$+\sum_{i=1}^{n}\int_{H_{i-1}}^{H_i}\int_0^{2\pi}\int_{r_p}^{\infty}\left\{G_{si}\phi_\theta^2\sin^2\theta + G_{si}\phi_r^2\cos^2\theta\right\}\left(\frac{dw_i}{dz}\right)\delta\left(\frac{dw_i}{dz}\right) r dr d\theta dz$$
$$-F_a\,\delta w_1\big|_{z=0} + M_a\delta\left(\frac{dw_1}{dz}\right)\Big|_{z=0}$$
$$+\sum_{i=1}^{n+1}\int_{H_{i-1}}^{H_i}\int_0^{2\pi}\int_{r_p}^{\infty}\Bigg\{\lambda_{si}w_i^2\cos^2\theta\left(\frac{\phi_r-\phi_\theta}{r}\right)$$
$$+\left(\lambda_{si}+2G_{si}\right)w_i^2\cos^2\theta\frac{d\phi_r}{dr}\Bigg\}\delta\left(\frac{d\phi_r}{dz}\right) r dr d\theta dz$$
$$+\sum_{i=1}^{n+1}\int_{H_{i-1}}^{H_i}\int_0^{2\pi}\int_{r_p}^{\infty}\Bigg\{\lambda_{si}\frac{w_i^2}{r}\frac{d\phi_r}{dr}\cos^2\theta + \left(\lambda_{si}+2G_{si}\right)\frac{w_i^2}{r^2}\left(\phi_r-\phi_\theta\right)\cos^2\theta$$
$$+G_{si}\frac{w_i^2}{r^2}\left(\phi_r-\phi_\theta\right)\sin^2\theta + G_{si}\frac{w_i^2}{r}\sin^2\theta\frac{d\phi_\theta}{dr}$$
$$+G_{si}\left(\frac{dw_i}{dz}\right)^2\cos^2\theta\,\phi_r\Bigg\}\delta\phi_r\, r dr d\theta dz$$
$$+\sum_{i=1}^{n+1}\int_{H_{i-1}}^{H_i}\int_0^{2\pi}\int_{r_p}^{\infty}\left\{G_{si}w_i^2\sin^2\theta\left(\frac{\phi_r-\phi_\theta}{r}\right) + G_{si}w_i^2\sin^2\theta\frac{d\phi_\theta}{dr}\right\}\delta\left(\frac{d\phi_\theta}{dz}\right) r dr d\theta dz$$
$$+\sum_{i=1}^{n+1}\int_{H_{i-1}}^{H_i}\int_0^{2\pi}\int_{r_p}^{\infty}\Bigg\{-\lambda_{si}\frac{w_i^2}{r}\frac{d\phi_r}{dr}\cos^2\theta - \left(\lambda_{si}+2G_{si}\right)\frac{w_i^2}{r^2}\left(\phi_r-\phi_\theta\right)\cos^2\theta$$
$$-G_{si}\frac{w_i^2}{r^2}\left(\phi_r-\phi_\theta\right)\sin^2\theta - G_{si}\frac{w_i^2}{r}\sin^2\theta\frac{d\phi_\theta}{dr}$$
$$+G_{si}\left(\frac{dw_i}{dz}\right)^2\sin^2\theta\,\phi_\theta\Bigg\}\delta\phi_\theta\, r dr d\theta dz = 0 \qquad [8]$$

Note, that the n^{th} layer is artificially split into n^{th} and $(n+1)^{th}$ layer. Further, in Eq. [8], G_{si} {= $E_{si}/(2\times(1+\nu_{si}))$} and λ_{si} {= $2G_{si}(1-\nu_{si})/(1-2\nu_{si})$} varies with strain at each point within the soil mass i.e., they are functions of the radial r and tangential θ coordinate (i.e., $G_{si} = G_{si}(r,\theta)$ and $\lambda_{si} = \lambda_{si}(r,\theta)$). For the circular soil domain of r_p below the pile base, the shear modulus is assumed to equal to the small-strain shear modulus (i.e., $G_{sn} = G_{sn0}$, see Eq. [1]).

3.4 Numerical solution of pile displacement

Performing integration by parts on the terms associated with $\delta(d^2w/dz^2)$ and $\delta(dw/dz)$, in Eq. [8], then collecting all the terms associated with δw and equating them to zero results in the differential equations of $w(z)$. Considering the terms associated with δw within the region $0 \le z \le L_p$, the governing differential equations of w is obtained, which is given by

$$E_p I_p \frac{d^4w_i}{dz^4} - 2t_i\frac{d^2w_i}{dz^2} + k_i w_i = 0 \qquad [9]$$

along with the relevant boundary conditions at different layer interface given by

$$E_p I_p \frac{d^3w_1}{dz^3} - 2t_1\frac{dw_1}{dz} = F_a \qquad [10]$$

$$E_p I_p \frac{d^2w_1}{dz^2} = -M_a \qquad [11]$$

$$w_i = w_{i+1} \qquad [12]$$

$$\frac{dw_i}{dz} = \frac{dw_{i+1}}{dz} \qquad [13]$$

$$\left[E_p I_p \frac{d^3w_i}{dz^3} - 2t_i\frac{dw_i}{dz}\right] = \left[E_p I_p \frac{d^3w_{i+1}}{dz^3} - 2t_{i+1}\frac{dw_{i+1}}{dz}\right] \qquad [14]$$

$$\frac{d^2w_i}{dz^2} = \frac{d^2w_{i+1}}{dz^2} \qquad [15]$$

$$\left[E_p I_p \frac{d^3w_n}{dz^3} - 2t_n\frac{dw_n}{dz}\right] = \sqrt{2k_n t_{n+1}}\,w_n \qquad [16]$$

$$\frac{d^2w_n}{dz^2} = 0 \qquad [17]$$

where the coefficients k_i and t_i are given by

$$k_i = \int_0^{2\pi}\int_{r_p}^{\infty}\left\{\left(\lambda_{si}+2G_{si}\right)\left(\frac{d\phi_r}{dr}\right)^2\cos^2\theta + 2\lambda_{si}\left(\frac{\phi_r-\phi_\theta}{r}\right)\frac{d\phi_r}{dr}\cos^2\theta \right.$$
$$+G_{si}r\left(\frac{d\phi_\theta}{dr}\right)^2\sin^2\theta + \left(\lambda_{si}+2G_{si}\right)\left(\frac{\phi_r-\phi_\theta}{r}\right)^2\cos^2\theta \qquad [18]$$
$$\left.+G_{si}\left(\frac{\phi_r-\phi_\theta}{r}\right)^2\sin^2\theta + G_{si}\left(\frac{\phi_r-\phi_\theta}{r}\right)\frac{d\phi_\theta}{dr}\sin^2\theta\right\} r dr d\theta$$

$$t_i = \begin{cases} \frac{1}{2}\int_0^{2\pi}\int_{r_p}^{\infty} G_{sn}\left(\phi_r^2\cos^2\theta+\phi_\theta^2\sin^2\theta\right) r dr d\theta; & i = 1,2,\ldots,n \\ \frac{1}{2}\int_0^{2\pi}\int_{r_p}^{\infty} G_{sn}\left(\phi_r^2\cos^2\theta+\phi_\theta^2\sin^2\theta\right) r dr d\theta + \frac{\pi}{2}r_p^2 G_{sn0}; & i = n+1 \end{cases} \qquad [19]$$

Note, that the parameters k_i and t_i are also functions of r and θ for a spatially varying G_{si} and λ_{si}.

For the domain below the pile base ($L_p \le z \le \infty$) the terms associated with δw_{n+1} in Eq. [8] are equated to zero. As w_{n+1} is not known *a priori* within $L_p < z < \infty$, $\delta w_{n+1} \neq 0$ because of which the integrand in the integral between $z = L_p$ and $z = \infty$ must be equal to zero. This gives the differential equation of w_{n+1}

$$2t_{n+1}\frac{d^2 w_{n+1}}{dz^2} - k_n w_{n+1} = 0 \qquad [20]$$

At infinite vertical distance down from the pile (i.e., at $z = \infty$) $w_{n+1} = 0$ (this makes the term associated with δw_{n+1} at $z = \infty$ equal to zero) and at the pile base (i.e., at $z = L_p$) $w_{n+1} = w_n$. Using these boundary conditions, an analytical solution of Eq. [20] is obtained as

$$w_{n+1} = w_n\big|_{z=L_p}\, e^{-\sqrt{\frac{k_n}{2t_{n+1}}}(z-L_p)} \qquad [21]$$

The differential equation governing pile displacement (Eq. [9]) is solved using the 1-D FD scheme. The FD form of Eq. [9] for various set of nodes (pile is discretized into a set of uniformly spaced nodes of spacing Δz (see Figure 3(b)) with a total number of nodes n (same as the number of soil layers) satisfying the boundary conditions at the pile-head (Eq. [10]-[11]) and at the pile-base (Eq. [16]-[17]) are given by

$$\left[\frac{2E_pI_p}{\Delta z^4}+\frac{4t_1}{\Delta z^2}+k_1\right]w_1 + \left[-\frac{4E_pI_p}{\Delta z^4}-\frac{4t_1}{\Delta z^2}\right]w_2 + \left[\frac{2E_pI_p}{\Delta z^4}\right]w_3 = \frac{2F_a}{\Delta z} - \frac{2M_a}{\Delta z^2} \qquad [22]$$

$$\left[-\frac{2E_pI_p}{\Delta z^4}-\frac{2t_2}{\Delta z^2}\right]w_1 + \left[\frac{5E_pI_p}{\Delta z^4}+\frac{4t_2}{\Delta z^2}+k_2\right]w_2 + \left[-\frac{4E_pI_p}{\Delta z^4}-\frac{2t_2}{\Delta z^2}\right]w_3 + \left[\frac{E_pI_p}{\Delta z^4}\right]w_4 = \frac{M_a}{\Delta z^2} \qquad [23]$$

$$\left[\frac{E_pI_p}{\Delta z^4}\right]w_{i-2} + \left[-\frac{4E_pI_p}{\Delta z^4}-\frac{2t_i}{\Delta z^2}\right]w_{i-1} + \left[\frac{6E_pI_p}{\Delta z^4}+\frac{4t_i}{\Delta z^2}+k_i\right]w_i + \left[-\frac{4E_pI_p}{\Delta z^4}-\frac{2t_i}{\Delta z^2}\right]w_{i+1} + \left[\frac{E_pI_p}{\Delta z^4}\right]w_{i+2} = 0 \qquad [24]$$

$$\left[\frac{E_pI_p}{\Delta z^4}\right]w_{i-2} + \left[-\frac{4E_pI_p}{\Delta z^4}-\frac{2t_i}{\Delta z^2}\right]w_{i-1} + \left[\frac{5E_pI_p}{\Delta z^4}+\frac{4t_i}{\Delta z^2}+k_i\right]w_i + \left[-\frac{2E_pI_p}{\Delta z^4}-\frac{2t_i}{\Delta z^2}\right]w_{i+1} = 0 \qquad [25]$$

$$\left[\frac{2E_pI_p}{\Delta z^4}\right]w_{i-2} + \left[-\frac{4E_pI_p}{\Delta z^4}-\frac{4t_i}{\Delta z^2}\right]w_{i-1} + \left[\frac{2E_pI_p}{\Delta z^4}+\frac{4t_i}{\Delta z^2}+\frac{2\sqrt{2k_it_{i+1}}}{\Delta z}+k_i\right]w_i = 0 \qquad [26]$$

Eqs. [22] and [23] are applicable to nodes 1 and 2 respectively, Eq. [24] is applicable to nodes $i = 3 - (n - 2)$, Eqs. [25] and [26] are applicable to nodes $i = (n - 1)$ and $i = n$, respectively. These FD equations form a system of linear equations whose solutions results in the pile displacement w_i at each node along the z-axis. Note, the small-strain shear modulus G_{s0} can be input at each node, which implicitly accounts for layering within the solution process.

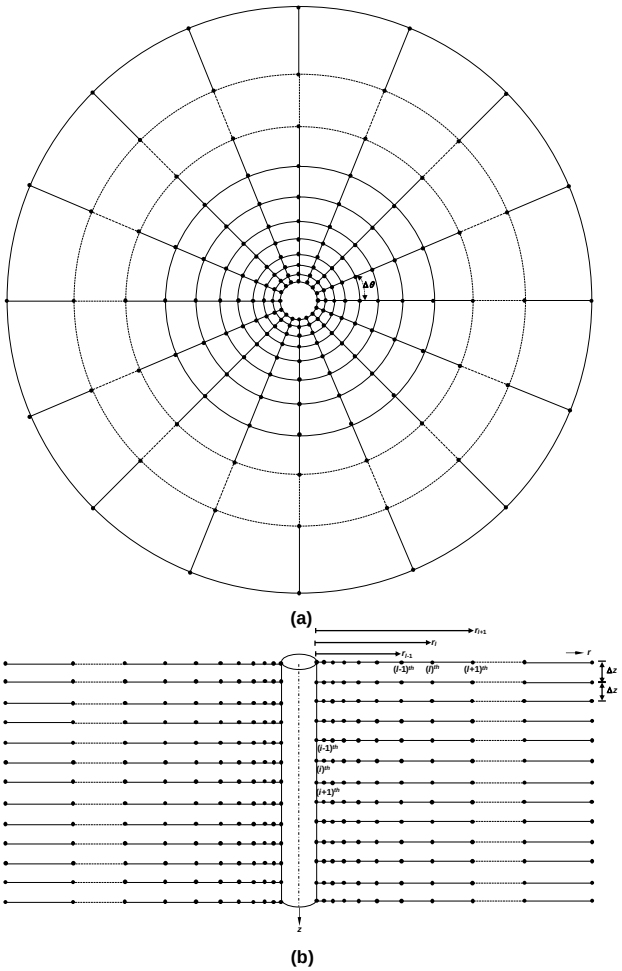

Figure 3. Finite difference discretisation of the pile-soil domain

3.5 Numerical solution of soil displacement

Referring to Eq. [8], collecting all the terms associated with $\delta\phi_r$, $\delta\phi_\theta$, $\delta(d\phi_r/dr)$, and $\delta(d\phi_\theta/dr)$ and further, performing integration by parts on the terms associated $\delta(d\phi_r/dr)$ and $\delta(d\phi_\theta/dr)$, an equation of the following form is obtained

$$\begin{aligned}
&\int_{r_p}^{\infty}\left\{-m_{s1}\frac{d^2\phi_r}{dr^2}-\frac{dm_{s1}}{dr}\frac{d\phi_r}{dr}-\frac{dm_{s3}}{dr}\left(\frac{\phi_r-\phi_\theta}{r}\right)+m_{s3}\left(\frac{\phi_r-\phi_\theta}{r^2}\right)+\frac{m_{s3}}{r}\frac{d\phi_r}{dr}\right.\\
&\left.-\frac{m_{s3}}{r}\left(\frac{d\phi_r}{dr}-\frac{d\phi_\theta}{dr}\right)+m_{s1}\left(\frac{\phi_r-\phi_\theta}{r^2}\right)+m_{s2}\left(\frac{\phi_r-\phi_\theta}{r^2}\right)+\frac{m_{s2}}{r}\frac{d\phi_\theta}{dr}+n_{s1}\phi_r\right\}\delta\phi_r\,dr\\
&+m_{s1}\frac{d\phi_r}{dr}\delta\phi_r\Big|_{r_p}^{\infty}+m_{s3}\left(\frac{\phi_r-\phi_\theta}{r}\right)\delta\phi_r\Big|_{r_p}^{\infty}\\
&\int_{r_p}^{\infty}\left\{-\frac{dm_{s2}}{dr}\frac{d\phi_\theta}{dr}-m_{s2}\frac{d^2\phi_\theta}{dr^2}-\frac{dm_{s2}}{dr}\left(\frac{\phi_r-\phi_\theta}{r}\right)-\frac{m_{s3}}{r}\frac{d\phi_r}{dr}-m_{s1}\left(\frac{\phi_r-\phi_\theta}{r^2}\right)\right.\\
&\left.-\frac{m_{s2}}{r}\left(\frac{d\phi_r}{dr}-\frac{d\phi_\theta}{dr}\right)+\frac{m_{s2}}{r}\frac{d\phi_\theta}{dr}+n_{s2}\phi_\theta\right\}\delta\phi_\theta\,dr\\
&+m_{s2}\frac{d\phi_\theta}{dr}\delta\phi_\theta\Big|_{r_p}^{\infty}+m_{s2}\left(\frac{\phi_r-\phi_\theta}{r}\right)\delta\phi_\theta\Big|_{r_p}^{\infty}=0
\end{aligned} \quad [27]$$

where

$$m_{s1}=\sum_{i=1}^{n}\int_{H_{i-1}}^{H_i}\int_0^{2\pi}\left(\lambda_{si}+2G_{si}\right)w_i^2\cos^2\theta\,r\,d\theta\,dz \quad [28]$$

$$m_{s2}=\sum_{i=1}^{n}\int_{H_{i-1}}^{H_i}\int_0^{2\pi}G_{si}w_i^2\sin^2\theta\,r\,d\theta\,dz \quad [29]$$

$$m_{s3}=\sum_{i=1}^{n}\int_{H_{i-1}}^{H_i}\int_0^{2\pi}\lambda_{si}w_i^2\cos^2\theta\,r\,d\theta\,dz \quad [30]$$

$$n_{s1}=\sum_{i=1}^{n}\int_{H_{i-1}}^{H_i}\int_0^{2\pi}G_{si}\left(\frac{dw_i}{dz}\right)^2\cos^2\theta\,r\,d\theta\,dz \quad [31]$$

$$n_{s2}=\sum_{i=1}^{n}\int_{H_{i-1}}^{H_i}\int_0^{2\pi}G_{si}\left(\frac{dw_i}{dz}\right)^2\sin^2\theta\,r\,d\theta\,dz \quad [32]$$

Collecting the terms associated with $\delta\phi_r$ and $\delta\phi_\theta$, setting the terms associated with $\delta\phi_r$ and $\delta\phi_\theta$ at $r = r_p$ and $r = \infty$ equal to zero (since the variations of ϕ_r and ϕ_θ are known at $r = r_p$ and $r = \infty$), and within the interval $r_p < r < \infty$ (since $\delta\phi_r \neq 0$ and $\delta\phi_\theta \neq 0$ as ϕ_r and ϕ_θ is not known *a priori* within $r_p < r < \infty$) a set of coupled differential equations for ϕ_r and ϕ_θ describing soil displacement are obtained.

$$\frac{d^2\phi_r}{dr^2}+\gamma_1\frac{d\phi_r}{dr}-\gamma_2\phi_r=\gamma_3\frac{d\phi_\theta}{dr}-\gamma_4\phi_\theta \quad [33]$$

$$\frac{d^2\phi_\theta}{dr^2}+\gamma_5\frac{d\phi_\theta}{dr}-\gamma_6\phi_\theta=-\gamma_7\frac{d\phi_r}{dr}-\gamma_8\phi_r \quad [34]$$

where

$$\gamma_1=\frac{1}{m_{s1}}\frac{dm_{s1}}{dr} \quad [35]$$

$$\gamma_2=\frac{1}{r^2}\left(\frac{m_{s1}+m_{s2}+m_{s3}}{m_{s1}}\right)-\frac{1}{r\,m_{s1}}\frac{dm_{s3}}{dr}+\left(\frac{n_{s1}}{m_{s1}}\right) \quad [36]$$

$$\gamma_3=\frac{1}{r}\left(\frac{m_{s2}+m_{s3}}{m_{s1}}\right) \quad [37]$$

$$\gamma_4=\frac{1}{r^2}\left(\frac{m_{s1}+m_{s2}+m_{s3}}{m_{s1}}\right)-\frac{1}{r\,m_{s1}}\frac{dm_{s3}}{dr} \quad [38]$$

$$\gamma_5=\frac{1}{m_{s2}}\frac{dm_{s2}}{dr} \quad [39]$$

$$\gamma_6=\frac{1}{r^2}\left(\frac{m_{s1}}{m_{s2}}\right)+\frac{1}{r\,m_{s2}}\frac{dm_{s2}}{dr}+\left(\frac{n_{s2}}{m_{s2}}\right) \quad [40]$$

$$\gamma_7=\frac{1}{r}\left(\frac{m_{s2}+m_{s3}}{m_{s2}}\right) \quad [41]$$

$$\gamma_8=\frac{1}{r^2}\frac{m_{s1}}{m_{s2}}+\frac{1}{r\,m_{s2}}\frac{dm_{s2}}{dr} \quad [42]$$

The coupled differential equations (Eqs. [33] and [34]) are solved simultaneously using a 1-D FD scheme. The discretized forms of the differential equations and the associated coefficients are given as

$$\begin{aligned}
&\frac{\phi_r^{l+1}-2\phi_r^l+\phi_r^{l-1}}{\left(r_{l+1}-r_l\right)\left(r_l-r_{l-1}\right)}+\gamma_1^l\frac{\phi_r^{l+1}-\phi_r^{l-1}}{\left(r_{l+1}-r_{l-1}\right)}-\gamma_2^l\phi_r^l\\
&=\gamma_3^l\frac{\phi_\theta^{l+1}-\phi_\theta^{l-1}}{\left(r_{l+1}-r_{l-1}\right)}-\gamma_4^l\phi_\theta^l
\end{aligned} \quad [43]$$

$$\begin{aligned}
&\frac{\phi_\theta^{l+1}-2\phi_\theta^l+\phi_\theta^{l-1}}{\left(r_{l+1}-r_l\right)\left(r_l-r_{l-1}\right)}+\gamma_5^l\frac{\phi_\theta^{l+1}-\phi_\theta^{l-1}}{\left(r_{l+1}-r_{l-1}\right)}-\gamma_6^l\phi_\theta^l\\
&=-\gamma_7^l\frac{\phi_r^{l+1}-\phi_r^{l-1}}{\left(r_{l+1}-r_{l-1}\right)}-\gamma_8^l\phi_r^l
\end{aligned} \quad [44]$$

where

$$\gamma_1^l=\frac{1}{m_{s1}^l}\frac{m_{s1}^{l+1}-m_{s1}^{l-1}}{r_{l+1}-r_{l-1}} \quad [45]$$

$$\gamma_2^l=\frac{1}{r_l^2}\left(\frac{m_{s1}^l+m_{s2}^l+m_{s3}^l}{m_{s1}^l}\right)-\frac{1}{r_l\,m_{s1}^l}\frac{m_{s3}^{l+1}-m_{s3}^{l-1}}{r_{l+1}-r_{l-1}}+\left(\frac{n_{s1}^l}{m_{s1}^l}\right) \quad [46]$$

$$\gamma_3^l = \frac{1}{r_l}\left(\frac{m_{s2}^l + m_{s3}^l}{m_{s1}^l}\right) \quad [47]$$

$$\gamma_4^l = \frac{1}{r_l^2}\left(\frac{m_{s1}^l + m_{s2}^l + m_{s3}^l}{m_{s1}^l}\right) - \frac{1}{r_l\, m_{s1}^l}\frac{m_{s3}^{l+1} - m_{s3}^{l-1}}{r_{l+1} - r_{l-1}} \quad [48]$$

$$\gamma_5^l = \frac{1}{m_{s2}^{l+1}}\frac{m_{s2}^{l+1} - m_{s2}^{l-1}}{r_{l+1} - r_{l-1}} \quad [49]$$

$$\gamma_6^l = \frac{1}{r_l^2}\left(\frac{m_{s1}^l}{m_{s2}^l}\right) + \frac{1}{r_l\, m_{s2}^l}\frac{m_{s2}^{l+1} - m_{s2}^{l-1}}{r_{l+1} - r_{l-1}} + \left(\frac{n_{s2}^l}{m_{s2}^l}\right) \quad [50]$$

$$\gamma_7^l = \frac{1}{r_l}\left(\frac{m_{s2}^l + m_{s3}^l}{m_{s2}^l}\right) \quad [51]$$

$$\gamma_8^l = \frac{1}{r_l^2}\left(\frac{m_{s1}^l}{m_{s2}^l}\right) + \frac{1}{r_l\, m_{s2}^l}\frac{m_{s2}^{l+1} - m_{s2}^{l-1}}{r_{l+1} - r_{l-1}} \quad [52]$$

where the superscript l represents the node number at a radial distance r_l from the pile edge and ($r_{l+1} - r_l$) or ($r_l - r_{l-1}$) is the discretization length (see Figure 3(b)). The FD discretization has its first node at the pile-soil boundary (i.e., at $r = r_p$) and is chosen sufficiently long and dense so as to allow proper attenuation of the displacement functions for accurate results.

Eqs. [42] and [43] when rewritten for nodes 2 through ($m - 1$) (i.e., excluding the 1st and the last (m^{th}) nodes at which the values of ϕ_r and ϕ_θ are known) generate two sets of simultaneous equations with each set containing $m - 2$ equations. These sets of equations can be represented in the matrix form as

$$\left[X^{\phi_r}\right]\{\phi_r\} = \left\{Y^{\phi_\theta}\right\} \quad [53]$$

$$\left[X^{\phi_\theta}\right]\{\phi_\theta\} = \left\{Y^{\phi_r}\right\} \quad [54]$$

where $\left[X^{\phi_r}\right]_{(m-2)\times(m-2)}$ and $\left[X^{\phi_\theta}\right]_{(m-2)\times(m-2)}$ are the tri-diagonal matrices with finite difference coefficients of the unknown vectors $\{\phi_r\}_{(m-2)\times 1}$ and $\{\phi_\theta\}_{(m-2)\times 1}$, respectively, and $\left\{Y^{\phi_r}\right\}_{(m-2)\times 1}$ and $\left\{Y^{\phi_\theta}\right\}_{(m-2)\times 1}$ are the corresponding right-hand side vectors containing terms with unknowns ϕ_θ and ϕ_r, respectively. As the right-hand vectors contain the unknowns ϕ_r and ϕ_θ, iterations are necessary to obtain their values. An initial estimate of ϕ_r is made and given as input to $\{Y^{\phi_r}\}$, and ϕ_θ is determined by solving Eq. [54]. The calculated ϕ_θ values are then given as input to $\{Y^{\phi_\theta}\}$ to obtain ϕ_r from Eq. [53]. The newly obtained values of ϕ_r are again used to obtain new values of ϕ_θ, and these iterations are continued until the convergence is reached. The criteria set for convergence are $\frac{1}{m}\sum_{l=1}^{m}\left|\phi_r^{l\,\text{previous}} - \phi_r^{l\,\text{current}}\right| \le 10^{-6}$ and $\frac{1}{m}\sum_{l=1}^{m}\left|\phi_\theta^{l\,\text{previous}} - \phi_\theta^{l\,\text{current}}\right| \le 10^{-6}$ where $\phi^{l\,\text{previous}}$ and $\phi^{l\,\text{current}}$ are the values of the ϕ functions (i.e., ϕ_r and ϕ_θ) at the l^{th} node for the previous and current iterations, respectively.

3.6 Solution algorithm

The soil parameters k and t which are functions of ϕ_r and ϕ_θ must be known to obtain w from the differential equation (Eq. [9]) describing the pile displacement. Moreover, the parameters γ_1-γ_8 (Eqs. [35]-[42]) must be known to obtain ϕ_r and ϕ_θ from Eqs. [33]-[34] and these parameters depend on w_i through m_{s1}, m_{s2}, m_{s3}, n_{s1}, and n_{s2} (Eqs. [28]-[32]). Therefore, the differential equation describing pile displacement w_i and soil displacement ϕ_r and ϕ_θ are coupled and an iterative algorithm is required to obtain a solution.

An initial guess of 1.0 is made for γ_1-γ_8 (Eqs. [45]-[52]) at each grid point (see Figure 3(a)) along r using which ϕ_r and ϕ_θ are determined using an iterative algorithm that satisfy the boundary conditions ϕ_r and $\phi_\theta = 1$ at $r = r_p$ and ϕ_r and $\phi_\theta = 0$ at $r = \infty$. After obtaining ϕ_r and ϕ_θ at each grid point, the strain components are calculated (using Eq. (5)) with which the secant shear modulus $G_s(r,\theta)$ are evaluated (using Eqs. [1] and [2]), at each grid point in the soil domain along r and θ and at each node along the z-axis (see Figure 3(b)). It is important to note that the induced displacement and strain varies at each point in the pile-soil domain because of which the secant shear modulus also varies at each point (because of the non-linear stress-strain behaviour of soil), which implies that the deformation induced in the soil mass because of pile movement renders the soil heterogeneous.

Using the calculated values of $G_s(r,\theta)$, ϕ_r and ϕ_θ, the values of k_i and t_i (Eqs. [18]-[19]) are obtained at each node along the pile length using the trapezoidal rule of integration where the integration is first performed along the r-direction with step length ($r_{l+1} - r_l$) or ($r_l - r_{l-1}$) at any tangential distance θ, followed by a subsequent integration over θ with step length $\Delta\theta$ (see Figure 3(a)). With the calculated values of k_i and t_i the pile displacement w_i and rotation dw_i/dz is evaluated (using Eqs. [22]-[26]) at different node points along the pile length with which the parameters m_{s1}, m_{s2}, m_{s3}, n_{s1}, and n_{s2} (Eqs. [28]-[32])) is evaluated numerically following the trapezoidal rule of integration, along the θ and z-direction. First, the integration is performed along θ at any radial distance r_l with a step length $r_l\Delta\theta$, the value of the integration obtained is further integrated along the z-direction with a step length Δz. After obtaining m_{s1}, m_{s2}, m_{s3}, n_{s1}, and n_{s2}, new values of γ_1-γ_8 are evaluated at each grid point and compared to the assumed initial values. If the differences are more than the prescribed tolerable limit of 0.001 at each grid point, the calculations described so far are repeated with the calculated values of γ_1-γ_8 as the new initial guesses. Iterations are continued until the values of γ_1-γ_8 between successive iterations fall below the prescribed limit at each grid point.

4 RESULTS

In order to verify the accuracy and computational efficiency of the present mathematical formulation, a comparison of the pile response obtained from the present analysis is done with the results of equivalent 3-D FE analyses using the nonlinear elastic relationships described by Eq. [1].

In the 3-D FE analysis (performed using ABAQUS), the pile and soil are modeled as a single cylindrical part with appropriate partitioning to represent the pile and soil separately, which ensures no slippage or separation between the soil and pile. The top soil surface is flush with the pile-head and the bottom soil surface is extended to a finite depth below the pile base. The horizontal radial extent of the soil domain is selected to be approximately 30 times the pile diameter from the pile axis. Different boundary conditions are prescribed at the boundaries of the model–all components of displacements are assumed to be zero along the bottom (horizontal) surface and two horizontal components are assumed to be zero along the outer, curved (vertical) surface of the soil domain. Eight-noded reduced integration (C3D8R) brick elements are used to model both the soil and pile domain. Concentrated force or moment is applied to a reference point at the pile head, to which all the nodes of the pile-head are connected. These loads (force/moment) are applied in several fixed increments.

The pile in the FE analysis is modeled as an elastic element whereas the soil is modeled using the nonlinear elastic relationship. In order to implement the nonlinear equations i.e., the variation of secant shear modulus of soil with the strain the ‘‘field variable (FV)” and the ‘‘user defined field” options, for the material definition in ABAQUS is used. In the simulations, the field variable is assigned as the Young’s modulus and the user-defined field (USDFLD) FORTRAN subroutine is written in Microsoft Visual Studio where Young’s modulus is made to vary with the evaluated value of the strain following Eq. [1] within the integration points of each element in the soil domain, for each load increment. In the FORTRAN code, the arrays of the strain components in each direction at each integration point within the soil elements are obtained using the GETVRM subroutine at the end of each increment. Then, the strain corresponding to Eq. [1] is calculated. Further, it is checked that if the strain is less than the minimum specified strain ($\varepsilon_{q0} < 10^{-5}$) within each element, then the initial Young’s modulus is specified to those elements; else for other elements, Young’s Modulus is evaluated using Eq. (1). The evaluated value of Young’s modulus for each element at the end of each increment is saved as a “solution dependent variable (SDV)” which is then used for the material definition at the integration points of each element of the soil domain in the next load increment. This (USDFLD) subroutine written is linked to the model developed in the ABAQUS Create job option and the analysis is performed in an Intel Fortran environment to get the outputs. Note, that for an accurate implementation of the variation of Young’s modulus, it is necessary that the size of the load increments and the size of the elements should be adequately chosen, based on convergence checks. For the problems solved, the pile-soil domain is discretized using a global seed of 1.0 and the applied load is divided into 40 increments.

Figures 4(a)-(b) show the comparison of the pile responses (head displacement w_h and rotation ψ_h) for an applied force and moment, respectively, obtained from the present analysis and 3-D FE analysis. The results are shown both for the soil modeled as an elastic and a nonlinear elastic material. The details of the pile-soil inputs are given in the figure itself. For the problems analyzed, the initial (elastic) shear modulus G_{s0} = 10 MPa with Poisson’s ratio ν_s = 0.2 is given as input in the present analysis. In the 3-D FE analysis, Young’s modulus of soil is made to vary with the deviatoric strain, therefore, the initial Young’s modulus E_{s0} {= $G_{s0} \times 2 \times (1 + \nu_s)$} = 24 MPa, is given as input. From the comparisons, it is evident that the present analysis predicts the pile response with a reasonable degree of accuracy. The difference in the nonlinear pile responses for the range of applied load is approximately less than 8%.

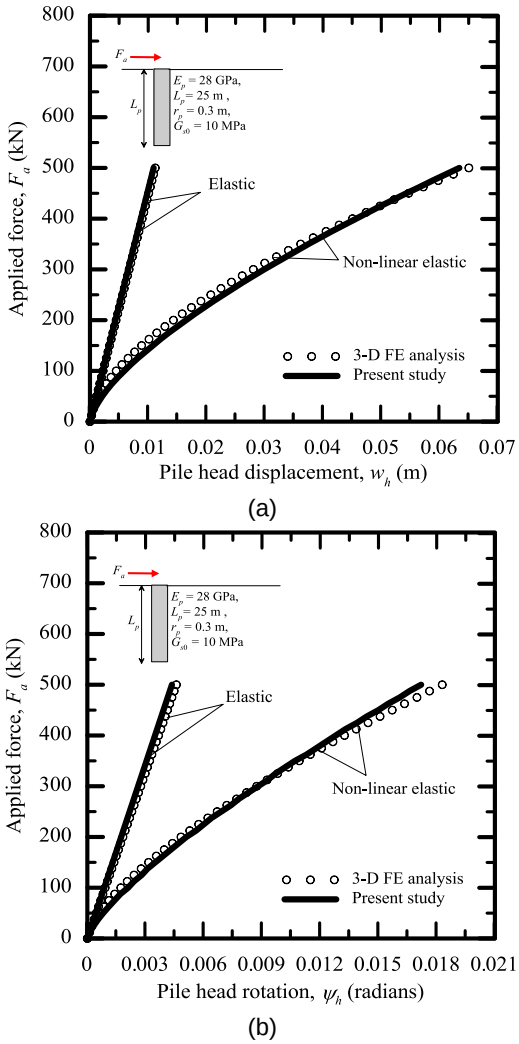

Figure 4. Comparison of pile response obtained from present and 3-D FE analysis for an applied force at the pile head (a) head displacement and (b) head rotation

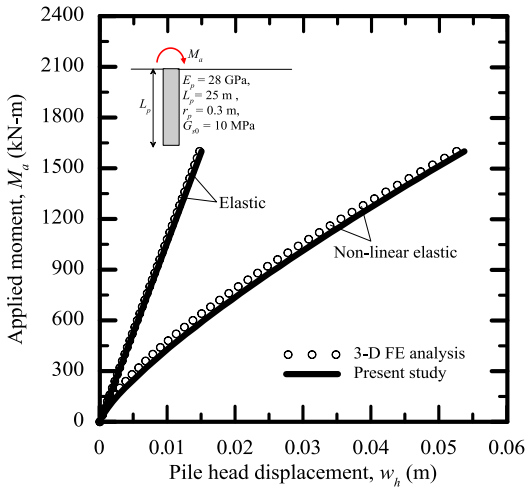

(a)

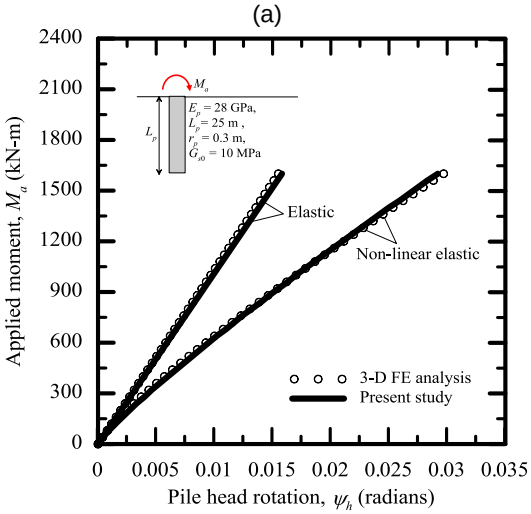

(b)

Figure 5. Comparison of pile response obtained from present and 3-D FE analysis for an applied moment at the pile-head (a) head displacement and (b) head rotation

The major advantage of the present framework is that it is computationally efficient in comparison to the 3-D FE framework for the same level of accuracy. Table 1 depicts the computational efficiency (CPU processing time for nonlinear analysis) from the present analysis (a MATLAB script is written) over the 3-D FE analysis (performed using ABAQUS) for the problems solved in computer with Intel® Core™ i5-3210M CPU @ 2.50 GHz and 8 GB RAM

Table 1. Computational time required for 3-D FE analysis and present analysis

Solved problems	3-D FE analysis (secs)	Present analysis, (secs)
Figures 5(a)-(b)	8685	337
Figures 6(a)-(b)	8777	356

5 CONCLUSIONS

A new continuum-based method is developed for the analysis of laterally loaded pile foundations embedded in a multilayered nonlinear elastic soil, subjected to a static force and moment at the pile-head. The soil displacement is considered to be a product of separable functions and the principle of virtual work is applied to obtain the governing differential equations describing the pile and soil displacements. An iterative algorithm is developed to obtain the pile and soil displacements in a 1-D FD scheme. The results obtained from the analysis are verified with the results of an equivalent 3-D FE analysis. A comparison of the CPU processing time is also shown to demonstrate the computational efficiency of the present analysis over 3-D FE analysis.

REFERENCES

Achmus, M., Kuo, Y. S., & Abdel-Rahman, K. (2009). Behavior of monopile foundations under cyclic lateral load. *Computers and Geotechnics*, *36*(5), 725-735.

American Petroleum Institute (API). (2011). "Recommended practice for planning, designing and constructing fixed offshore platforms—Working stress design." *API Recommended Practice* (*RP 2A-WSD*), 21st ed., Washington DC.

Baguelin, F., Frank, R., & Said, Y. H. (1977). Theoretical study of lateral reaction mechanism of piles. *Geotechnique*, *27*(3), 405-434.

Basu D, Salgado R, Prezzi M (2009). Acontinuum-based model for analysis of laterally loaded piles in layered soils. *Geotechnique*; 59(2):127-140.

Gupta, B. K., & Basu, D. (2017). Analysis of laterally loaded short and long piles in multilayered heterogeneous elastic soil. *Soils and Foundations*, *57*(1), 92-110.

Kooijman, A. P. (1989). Comparison of an elastoplastic quasi three-dimensional model for laterally loaded piles with field tests. *Numerical models in geomechanics-NUMOG III*, 675-682.

Nogami, T., & Novak, M. (1977). Resistance of soil to a horizontally vibrating pile. *Earthquake Engineering & Structural Dynamics*, *5*(3), 249-261.

O'Neill, M. W., Reese, L. C. & Cox, W. R. (1990). Soil behavior for piles under lateral loading. *Proc. 22nd Offshore Tech. Conf.*, Houston, Texas, 3, 279-287

Osman, A. S., White, D. J., Britto, A. M., & Bolton, M. D. (2007). Simple prediction of the undrained displacement of a circular surface foundation on non-linear soil. *Géotechnique*, *57*(9), 729-737.

Reese, L. (1975). Field testing and analysis of laterally loaded piles in stiff clay. In *Proc. 7th Offshore Technology Conference, Houston, Texas, 1975* (pp. 672-690).

Trochanis, A. M., Bielak, J., & Christiano, P. (1991). Three-dimensional nonlinear study of piles. *Journal of Geotechnical Engineering*, *117*(3), 429-447.

Zhang, L., & Ahmari, S. (2013). Nonlinear analysis of laterally loaded rigid piles in cohesive soil. *International Journal for Numerical and Analytical Methods in Geomechanics*, *37*(2), 201-220.